Batteries & Supercaps

Chemistry Europe
European Chemical Societies Publishing

Reprint

WILEY-VCH

doi.org/10.1002/batt.202000238

High-Performing Li-Ion Battery with "Two Cathodes in One" of Sulfur and $LiFePO_4$ by Strategies of Mitigation of Polysulfide Shuttling

Juan David Garay-Marín,[a] Enrique Quiroga-González,*[a] Lorena Leticia Garza-Tovar,[b] Florian Reuter,[c] Christian Kensy,[c] Holger Althues,[c] and Stefan Kaskel[c]

This work reports on further development of the concept "two cathodes in one" for lithium-ion batteries. The cathodes are composed of $LiFePO_4$ (high power) and sulfur (high gravimetric capacity), allowing high discharging rates as well as high gravimetric capacities, which are especially attractive for numerous existing applications. In this study, different strategies have been tested to reduce polysulfide shuttling in batteries with these cathodes, greatly improving their performance. Batteries which were assembled with electrolyte mixtures of tetramethylsulfone and 1,1,2,2-tetrafluoroethyl-2,2,3,3-tetrafluoropropyl ether (TMS/TTE) show significantly better performance than with the typical electrolyte composition used for Li–S batteries. Moreover, various carbons with different pore size distributions in the C/S composite were mixed with $LiFePO_4$ in an electrode reaching high discharge capacities (72% of the theorical composite capacity) and stable Coulombic efficiency of 99%. As a result, an improved active material utilization is observed, confirming its possible application as a commercial battery cathode.

1. Introduction

Large-scale applications such as renewable energy storage and effective electromobility (transportation), demand high-tech improvements in storage technology of lithium-ion batteries.[1,2] However, there is no commercial battery with high energy density and high power at the same time. In a previous work, a $LiFePO_4$-Sulfur composite has emerged as a promising cathode material, under the concept "two cathodes in one".[3] The system worked without reaction between both active materials during the first cycles, when LiTFSI in ether-based solvents was used as electrolyte and $LiFePO_4$ was coated with carbon. However, it is necessary to develop a stable electrolyte for this specific battery to obtain the advantages of both cathode materials.

Lithium ion batteries with transition metal oxides, such as $LiMn_2O_4$ and $LiCoO_2$, have been extensively examined as cathode materials. But, due to its high charge rate capability and good thermal stability at high temperature with a theoretical specific capacity of 170 $mAh\,g^{-1}$, lithium iron phosphate, $LiFePO_4$, is considered one of the best candidates for a variety of applications.[4,5] Furthermore, it has attracted considerable attention in the energy storage industry due to its low cost, environmental attributes, safety and predominantly, its high instantaneous power delivered near to 3.45 V versus Li/Li^+.[6–7] Nevertheless, currently the theoretical capacity of the compound is too low to satisfy applications demanding high energy density.[8,9] Correspondingly, lithium-sulfur (Li–S) batteries are a promising energy storage technology and could be an option to replace lithium ion batteries due to its gravimetric energy density and lower cost.[10] However, dissolution of lithium polysulfide intermediates and shuttle effect in conventional Li–S electrolytes need to be addressed for practical application. Polysulfide shuttle is one of the key challenges to the development of Li–S batteries, due to plenty of chemical and electrochemical side-reactions, redistribution and irreversible deposition of Li_2S/Li_2S_2 on the metallic lithium surface which leads to the rapid capacity fading during cycling.[11–15]

High power and high gravimetric capacity are required by battery systems to satisfy the demands of nowadays advanced technologies, for instance electric/hybrid vehicles (EV/EHV) or for stationary energy storage systems. In the proposed $LiFePO_4$–S composite, the same issues presented for the Li–S system must be solved as well. Li–S batteries are cycled at very modest C-rates (C/10 in average) to retain the capacity; the reason is primarily limitations of mass transport both in the electrolyte and on the electrolyte/electrode interface.[16] Despite the fact $LiFePO_4$ has low gravimetric capacity, it could provide the required power when S is limited at high C rates. In the past, sulfur has been used just in small amounts as dopant, changing the properties of $LiFePO_4$.[8,12,17] Even when there are efforts combining $LiFePO_4$ and S in a battery, they aimed to use either sulfur or $LiFePO_4$, with the other material improving certain characteristic (electronic transport, polysulfide retention, ion transport, etc.).[12,18,19,20] In none of the works, the cathode

[a] J. D. Garay-Marín, Dr. E. Quiroga-González
Institute of Physics
Benemérita Universidad Autónoma de Puebla
72570 Puebla, México
E-mail: equiroga@ieee.org
[b] Dr. L. L. Garza-Tovar
Faculty of Chemical Sciences
Universidad Autónoma de Nuevo León
66455 San Nicolás de los Garza N.L., México
[c] F. Reuter, C. Kensy, Dr. H. Althues, Prof. Dr. S. Kaskel
Fraunhofer Institute for Material and Beam Technology (IWS)
01277 Dresden, Germany

was conceived with two active materials ($LiFePO_4$-Sulfur composites as cathode) from the first charge/discharge cycle. The first work on this concept is "Two Cathodes in One for Li ion batteries: voltammetric study of a composite cathode of sulfur and $LiFePO_4$".[3]

Furthermore, preceding studies have discovered that 1,3-dioxolane solutions (DOL) are particularly well suited for Li anodes in secondary batteries, due to the unique surface chemistry of lithium electrodes in these solutions that partially prevent dendrite formation and allow facile Li-ion transport through them.[21,22] However, DOL solvent is not adequate for sulfur cathodes, therefore it required electrolyte modifications with different solvents, additives and Li salts. The shuttle mechanism is largely avoided by enhancing the passivation of the Li anodes, using solutions of LiTFSI in DME/DOL with $LiNO_3$.[23] Lithium nitrate is commonly used as an additive, which can form a solid electrolyte interface (SEI) on the Li metal anode, thus suppressing side reactions between polysulfides and metallic lithium anode.[24,–25] However, $LiNO_3$ is irreversible consumed during plating of Li metal and finally depleted.[25]

Recently, an innovative electrolyte composition was introduced for Li–S batteries and Lithium-ion batteries, consisting of 1.5 M LiTFSI, lithium bis(trifluoromethanesulfonyl)imide in a mixture of TMS/TTE in a 1:1 volume ratio, which greatly suppresses high order polysulfide dissolution (and indirectly suppresses polysulfide shuttling), but provides reasonably good solubility of the lithium salt, improving the cycle life of the cell.[26–27]

Finally, most recent efforts on Li–S batteries are dedicated to developing appropriate host materials structures to reduce the dissolution of polysulfides. Usually, an approach to confine polysulfides within the pores structure is employed. These host materials involve mesoporous carbon, hollow carbon spheres, graphene, hollow carbon nanofibers,[28–34] transition metal oxides or carbides.[34–36] Another approach was demonstrated with highly porous nitrogen doped carbons, caused by interaction of nitrogen species with lithium polysulfides intermediates improving the cycle stability by suppression of shuttle mechanism.[37]

In this work, different strategies used in common Li–S batteries were applied for controlling the diffusion of high order polysulfides (separators, conductive additives, binders, etc.). Moreover, various electrolyte compositions as well as different carbon structures are analyzed to improve the performance of this new cathode material. The cells are utilized in the whole operation potential window of the composite cathode, 1.50–3.85 V vs Li/Li^+. The main objective of this investigation is the application of this novel composite cathode as working electrode of a real-life battery offering benefits that common batteries could not comply.

2. Results and Discussion

2.1. Electrochemical Characterization of $LiFePO_4$–S-Corncob Composites with Different Electrolytes

2.1.1. Tests with Standard Electrolyte (DME/DOL) for Li–S Batteries

Initially in this work, both active materials ($LiFePO_4$/C and S/C) were examined separately with 1.0 M LiTFSI in DME/DOL electrolyte and $LiNO_3$ additive, with a polypropylene (PP) separator (Figure 1). In the S-Corncob half cells (Figure 1a) two characteristic plateau profiles are observed during discharge process, first one corresponding to the conversion of solid sulfur S_8 to high-order lithium polysulfides (Li_2S_x, $6 \leq x \leq 8$) which are formed at approximately 2.35 V and the second one, corresponds to the transition of low-order lithium polysulfides (Li_2S_{4-2}) to Li_2S located at 2.1 V. The voltage profile shows a plateau around 2.3 V, indicating a reversible reaction of Li with sulfur, in delithiation process.[12–14,38,39]

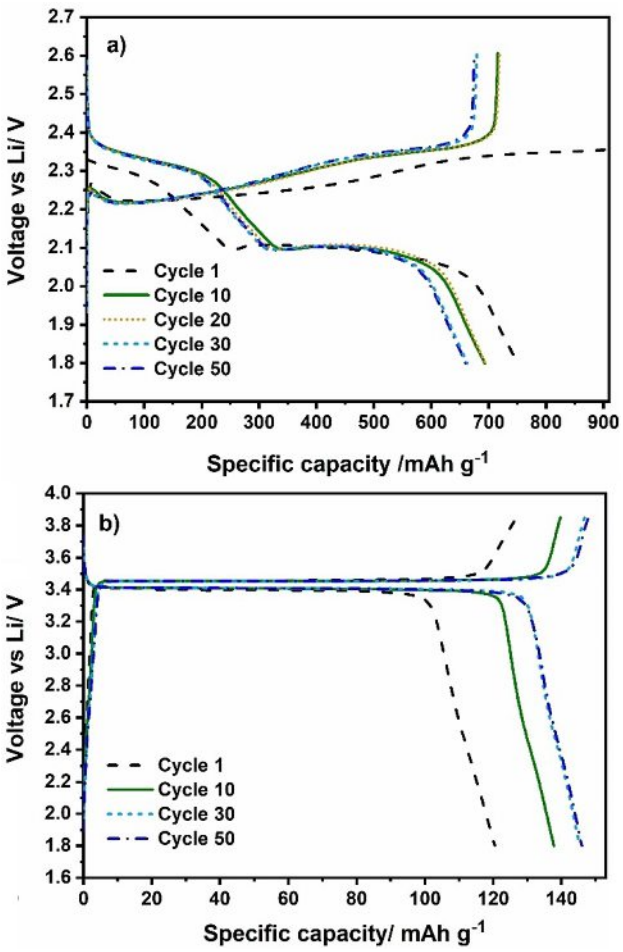

Figure 1. Charge/discharge curves of a) S/corncob composite with sulfur loading of approx. 2.77 mg cm^{-2} (carbon derived from biomass) and b) $LiFePO_4$ (3.16 mg cm^{-2}), with 1.0 M LiTFSI in DME/DOL with 0.25 M $LiNO_3$ additive.

Furthermore, $LiFePO_4$ was tested in the same electrolyte system and showed lithiation and delithiation plateaus at ~3.4 and 3.45 V which are similar to previous reports.[6,7] During cycling, the capacity increases between first and 30th cycle to more than 140 mAh g^{-1} and remains constant until 50th cycle.

With the purpose to test these two materials together as cathode, the composite, a paste electrode of the composite $LiFePO_4$–S-Corncob with an enhanced active material content (80 w%) was prepared and tested in DME/DOL electrolyte, similarly to the previous publication of the group, where the concept "two cathodes in one" was introduced.[3] Figure 2 shows a cyclic voltammetry curve (at cycle number 2) of a half-cell of $LiFePO_4$–S–C (Corncob)||Li. As can be observed, the lithiation and delithiation peaks of both active materials are present. The peaks B–C are attributed to lithiation of sulfur and peak Y to its corresponding delithiation.[12–14] On the other hand, peak A relates with the lithiation of $LiFePO_4$, while the peak Z comes from the delithiation of this material.[6,7]

According to the results presented in Figure 1, modest capacities and relatively good stability are observed for individually active material. Nevertheless, if the combination of $LiFePO_4$ and Sulfur is analyzed as composite in a half cell, it shows poor stability in galvanostatic cycling (Figure 3a) and suddenly increases or decreases in capacity (for example in cycle 30). This changing capacity behavior is related to polysulfide shuttling, since the electrolyte presents high polysulfide solubility[25] and the hierarchical porosity of corncob carbon is not enough to retain sulfur within the pores. Moreover, in some cycles (Cycle: 1–3, 5–8, 16, 27, 50) the delithiation voltage of $LiFePO_4$ (3.4 V) is reached and in others was not, which can be a result of the shuttle effect. However, the non-utilization of $LiFePO_4$ does not explain the capacity reduction of 300 mAh g^{-1}. Therefore, the experimental conditions, especially the voltage window for the galvanostatic testing is adapted to understand these phenomena (the materials were activated independently). Figures 3b and 3c show voltage profiles of $LiFePO_4$–S-Corncob composite between 1.60–2.80 V (lithiation/delithiation of sulfur) and 3.00–3.85 V (lithiation/delithiation of $LiFePO_4$) during various cycles. Both materials exhibit an enhanced gravimetric capacity, particularly sulfur. The increment of capacity of sulfur may be produced by the enhancement of electronic transport by the addition of $LiFePO_4$.[12,19] On the other hand, the increment in capacity of $LiFePO_4$ may be originated by the presence of sulfur in the electrolyte. The batteries showed improved electrochemical performance after the increase of lattice parameters of $LiFePO_4$ structure due to doping with sulfur (ionic radius of S^{2-} is larger than O^{2-}), which facilitates the transport of Li ions in the channels of the structure.[8,17] However, in the first cycles (from cycle 1 to cycle 5) the cut-off voltage for charging is not achieved for the sulfur electrode, illustrating the strong shuttle effect by infinity charge at almost constant voltage (as can be seen in Figure 3b). A similar behavior has been reported in previous investigation of Li–S batteries.[42] Then, in the next cycles the effect is less pronounced, but the charge capacities remain larger than their corresponding discharge capacities.[12,25,40–42] Finally, the performance is almost stabilized after 10 cycles.

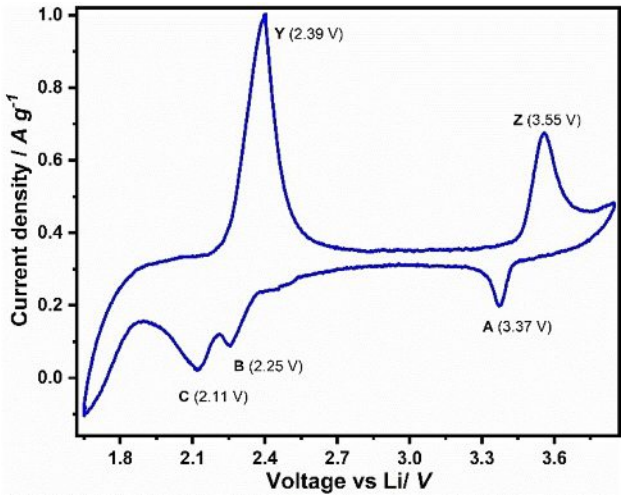

Figure 2. Cyclic voltammetry of $LiFePO_4$–S cathodes with carbon-coated $LiFePO_4$ and sulfur infiltrated in porous carbon with 0.7 M LiTFSI in DME/DOL with 0.25 M $LiNO_3$ additive, at a scan rate of 80 μV s^{-1}.

2.1.2. Test with TMS/TTE Electrolyte

In the search for an electrolyte that improves a better performance with the $LiFePO_4$–S compound, it is proposed to investigate LiTFSI electrolyte with different solvents. LiTFSI salt in TMS/TTE blended solvents provide reduced solubility for lithium polysulfides, resulting in high coulombic efficiency (CE). TTE is an excellent solvent for suppressing polysulfide dissolution with a boiling point of 93 °C.[22] Sulfolane solvent (TMS) has low toxicity with a permittivity of $\varepsilon = 42.12$ at 40 °C[43] and a donor number of 14.7. The dielectric permittivity of a solvent determines the capability to dissolve lithium polysulfides.[44]

Both active materials are examined individually, now a PE separator was used with this electrolyte, the charge/discharge profiles of $LiFePO_4$–C and S–C (sulfur infiltrated in active carbon derived from biomass) are shown in Figure 4. The performance of S–C composite is presented in Figure 4a. A remarkable overpotential during lithiation is observed during 50 cycles, the slope of the curve is changing drastically whereas the activation process should be developed at constant voltage. The S–C cathode exhibits poor gravimetric capacity in both charge and discharge curves. This could be caused trough poor wettability due to high viscosity of the TMS/TTE electrolyte resulting in a high polarization and increased cell resistance.[26] In contrast, $LiFePO_4$-electrode shows relatively good performance and stability according to the theoretical capacity of 170 mAh g^{-1}. Also, a behavior of increasing capacity over cycles in $LiFePO_4$ is determined in figure 4b, the plateaus of lithiation and delithiation are comparable to the reported potentials in literature.[6,7] This increase of capacity could be associated with the stabilization of half-cell battery and enhanced wettability of the cathode during cycling.

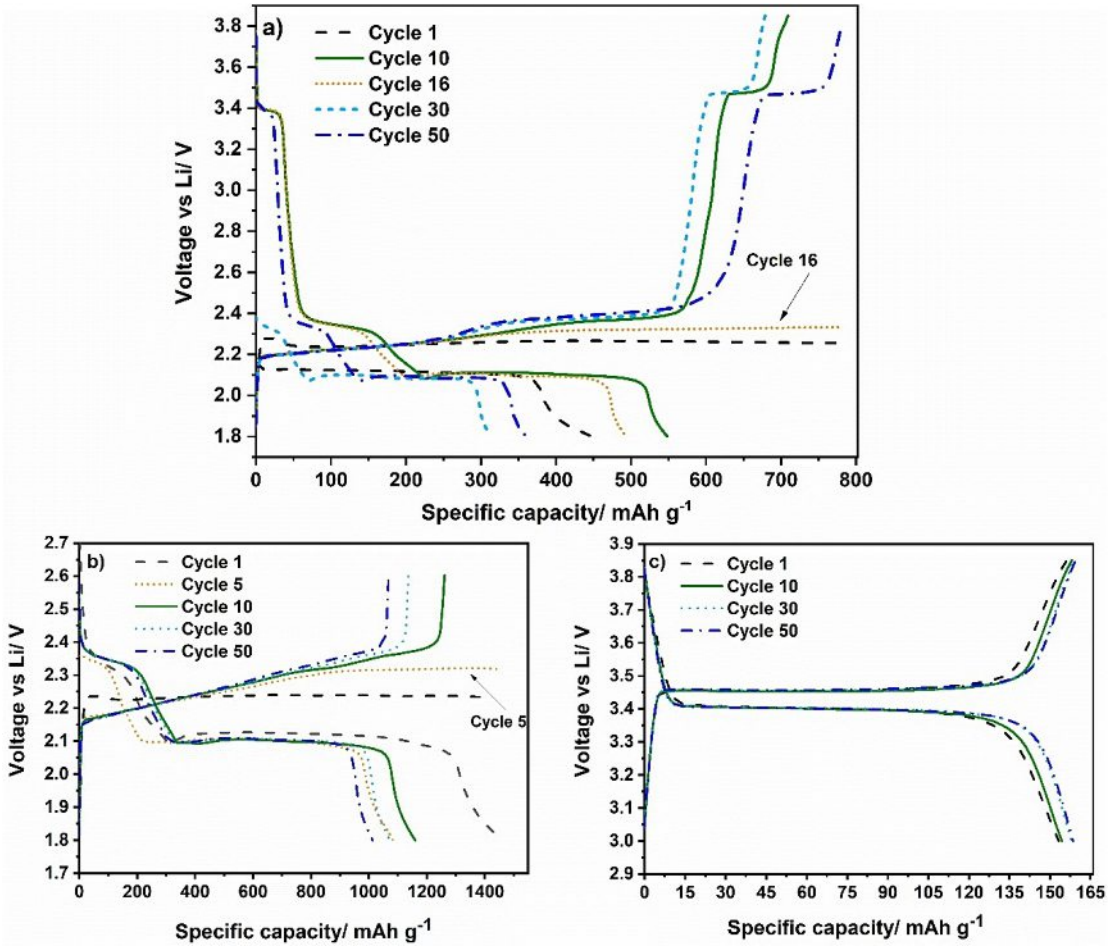

Figure 3. Charge/discharge curves of $LiFePO_4$–S composite cycled using 1.0 M LiTFSI in DME/DOL with 0.25 M $LiNO_3$ under different voltage windows: a) 1.8–3.85 V, b) 1.8–2.6 V (working voltage range of sulfur) and c) 3–3.85 V (working voltage range of $LiFePO_4$). Gravimetric capacity of b) and c) were calculated using just the mass of the activated material (2.27 mg cm^{-2} of composite loading) with the purpose to compare these results with the obtained when they were tested separately.

Figure 5a shows charge/discharge curves of the $LiFePO_4$–S-Corncob composite with TMS/TTE electrolyte. Prior to the electrochemical testing, coin cells were treated at 32 °C for 2 hours. In the first cycles total capacity of the composite of 700 mAh g^{-1} is observed and both lithiation and delithiation plateaus are determined at the expected potentials for sulfur (~ 2.3 V and 2.1 V). $LiFePO_4$ is electrochemically addressed, however, a slight over-potential is observed for the delithiation process at ~3.5 V. On the other hand, Sulfur electrode shows a good cycle performance and enhanced stability in the first cycles compared to the previous results with DME/DOL electrolyte. Figure 5b depicts a stable CE of 95% after the first 10 cycles. The achieved capacity is promising, and close to the calculated theoretical gravimetric capacity of 972 mAh g^{-1}_{Comp} for the composite. The first discharge plateau is reduced, which is related to long chain polysulfides, due to restricted polysulfide solubility in TMS/TTE electrolyte, suppressing degradation caused by the shuttling effect.[26] However, significant fading is presented after cycle 10 probably due to the natural structure of carbon derived from biomass and pore blocking effect.

2.2. Application of Various Carbonaceous Scaffolds for Sulfur

In order to improve the performance of the battery and since there was still migration of polysulfides, different conductive scaffolds are investigated as cathode material. Firstly, a commercially available microporous carbon (Micropore) is analyzed. Figure 6a illustrates the charge/discharge curves of the $LiFePO_4$–S-Micropore composite with TMS/TTE electrolyte, three different plateaus are observed in discharge process, first and second plateaus at ~2.3 and 2.0 V showing low gravimetric capacity and the third plateau at ~1.8 V provides the rest of the total capacity. Moreover, an over-potential for lithiation of sulfur is determined probably due to polarization effect of the electrolyte system. Furthermore, $LiFePO_4$ capacity contribution in the total capacity of the composite is increasing up to 50 cycles and its plateaus are present without significant over-potential and with more than 97% of CE, as can be seen in figure 6b.

Additionally, Ketjenblack, an often-utilized reference carbon material is used as host material. Figure 7a displays charge/discharge profiles of $LiFePO_4$–S-Ketjen composite. In contrast to

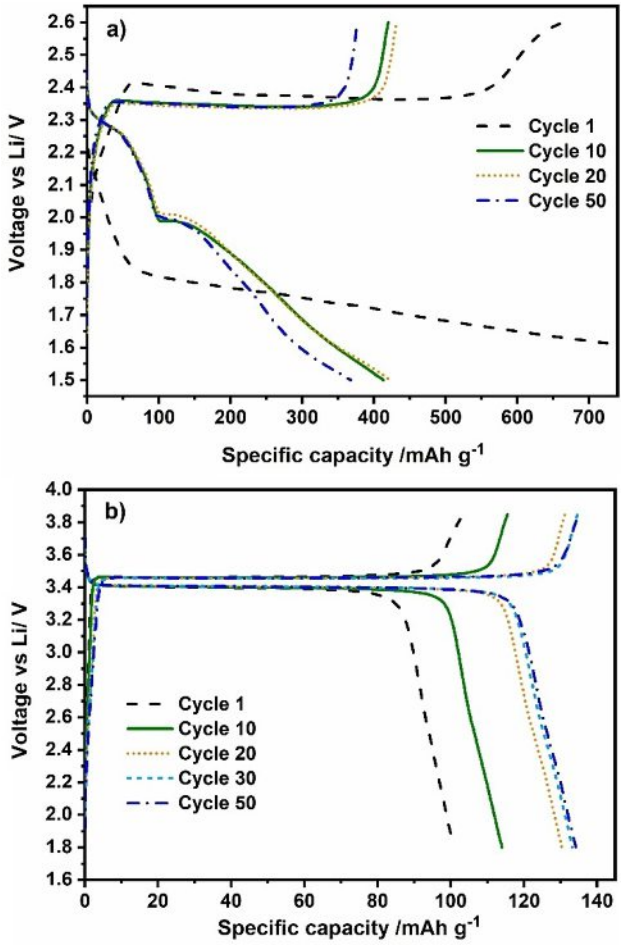

Figure 4. Charge/discharge curves of a) S–C with sulfur loading of approx. 2.77 mg cm^{-2} (carbon derived from biomass) and b) $LiFePO_4$–C with 1.5 M LiTFSI in TMS/TTE.

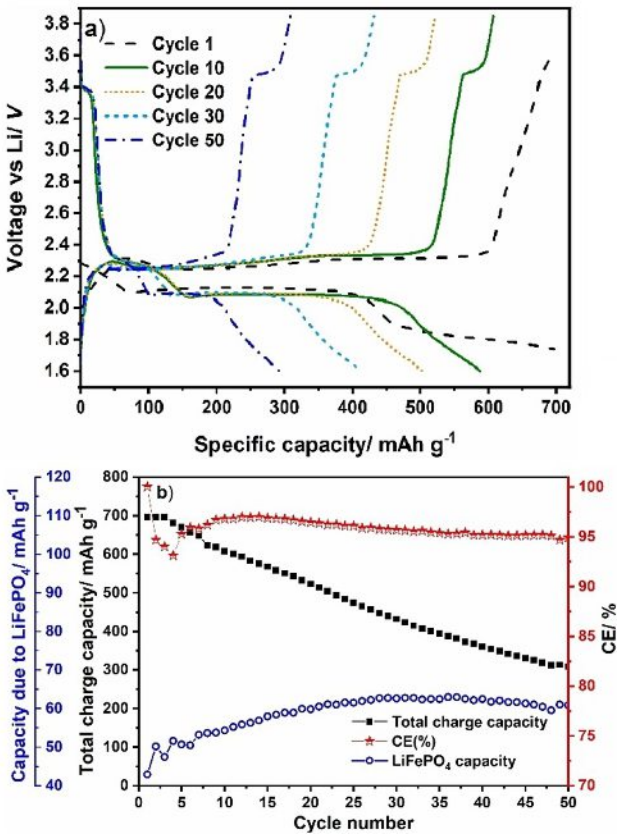

Figure 5. a) Charge/discharge curves and b) Galvanostatic cycling performance of $LiFePO_4$–S composite (sulfur infiltrated in carbon derived from biomass) with 1.5 M LiTFSI in TMS/TTE. $LiFePO_4$ capacity is calculated as indicated in experimental section. Active composite material loading of 2.27 mg cm^{-2}.

the previous analyzed cathode materials an enhanced cycle performance as well as coulombic efficiency (99%) is observed. However, a slight over-potential for the two discharge plateaus at ~2.20 V and 2.0 V is determined. The first plateau of high order polysulfides (Li_2S_x, $6 \leq x \leq 8$) is longer than expected (the capacity obtained should be considerably reduced).[26] High sulfur utilization is caused by the inter-particle porosity of Ketjenblack (carbon particles are agglomerated and generate inter-particular mesopores). Therefore, hierarchical pore structure seems to be promising for the active material utilization.

Figure 8 illustrates d*Q*/d*V* curves of various $LiFePO_4$–S cathodes with 1.0 M LiTFSI in DME/DOL and 1.5 M in TMS/TTE electrolyte. Those were calculated from charge/discharge curves of voltage (*V*) vs capacity (*Q*), reported in this investigation, considering cycle 10 for all tested cells. Electrochemical processes in battery cells can be illustrated in detail with help of d*Q*/d*V* slopes to analyze the existence of phenomena upon charge/discharge cycling, even with more accuracy than cyclic voltammetry.

Figure 8a corresponds to the lithiation and delithiation of Corncob $LiFePO_4$–S cathode with DME/DOL electrolyte. This cathode material exhibits the typical signals of both active materials. For the sulfur, peaks at 2.34 and 2.10 V related to the lithiation and peaks at 2.23 and 2.37 V associated to delithiation are observed. It is noticeable that peak B at ~2.34 V, related to high order polysulfides, exhibits lower over-potential compared to the other samples with different electrolyte solvents. Sharp peaks related to charge and discharge of $LiFePO_4$ are well defined at 3.47 V and 3.39 V, respectively. As the signals of the corresponding utilization are well distinctive, this cell is used as reference for the following carbon material comparison.

Figure 8 b, c and d show the lithiation and delithiation processes of different carbon $LiFePO_4$–S composite in TMS/TTE solvent. In figure 8b, $LiFePO_4$–S-Corncob composite reveals comparable peaks compared to the DME/DOL reference. However, a slightly over-potential is observed for the lithiation of Sulfur at 2.28 V and 2.08 V (DME/DOL: 2.34 V and 2.10 V). Interestingly, the delithiation peaks show no polarization (2.25 V and 2.34 V). For $LiFePO_4$ utilization broad peaks are observed.

Figure 8c shows peaks of $LiFePO_4$–S-Micropore composite. The first two signals for sulfur are at similar voltage positions compared to $LiFePO_4$–S-Corncob composite. However, an additional peak for the lithiation (M at 1.76 V) as well as the delithiation peak (M* at 2.70 V) are observed. The S/C composite exhibits two conversion mechanism, typical solid-

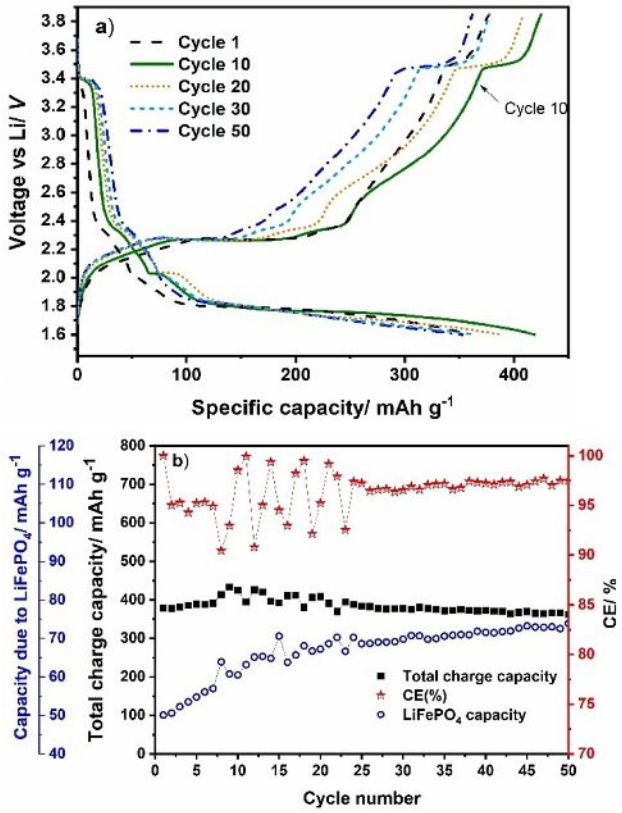

Figure 6. a) Charge/discharge curves and b) Galvanostatic cycling performance of $LiFePO_4$—S-Micropore composite with 1.5 M LiTFSI in TMS/TTE. Active composite material loading of 2.12 mg cm^{-2}.

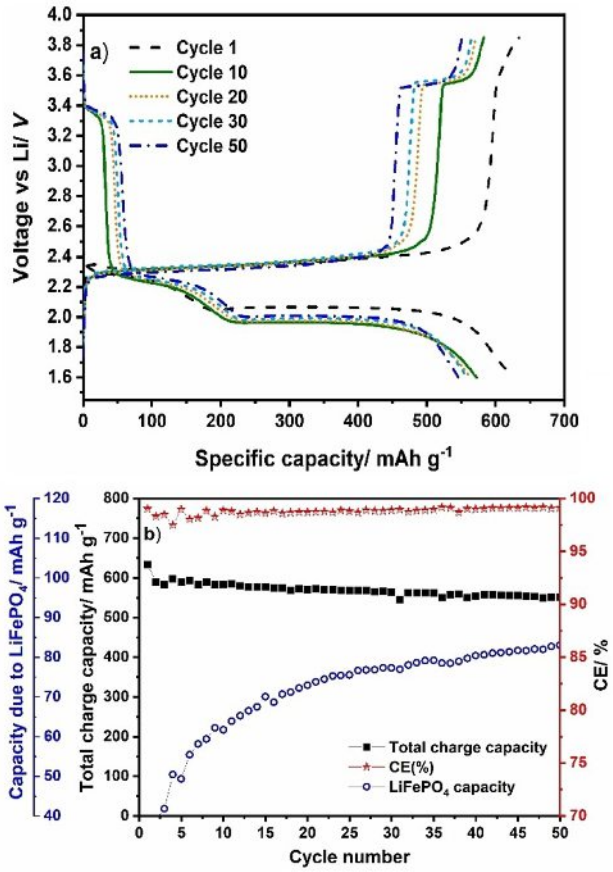

Figure 7. a) Charge/discharge curves and b) Galvanostatic cycling performance of $LiFePO_4$—S-Ketjen composite (sulfur infiltrated in ketjenblack carbon) with 1.5 M LiTFSI in TMS/TTE. Active composite material loading of 2.62 mg cm^{-2}.

liquid-solid (voltage profiles with two plateaus) and quasi-solid-state conversion QSS (single plateau). This mix behavior could be assigned to a relatively good wettability in micropores between 1–2 nm and solvent deficient conditions in narrow micropores lower than 1 nm (QSS conversion).[45,46,47] Furthermore, one intense oxidation peak (*) at 2.26 V is noticed, probably related to the high polarization produced by the above-mentioned effect in micropores, before the beginning of the second peak of delithiation process located at 2.34 V.

The d*Q*/d*V* curve of $LiFePO_4$—S-Ketjen composite is presented in figure 8d, all peaks reveal slightly shift to higher potentials compared to the other carbon materials. Moreover, a remarkable polarization is observed between lithiation and delithiation of sulfur peaks C (1.97 V) and X (2.33 V). During delithiation process of $LiFePO_4$ the peak Z is shifted to 3.56 V, probably affected by the enhancement of resistivity of the complete cell during cycling. Nevertheless, $LiFePO_4$—S-Ketjen composite shows enhanced cycle performance after 50 cycles with CE of 99% and a fading per cycle of about 0.264%, resulting in a higher final gravimetric capacity among the samples (Table 1).

After the analysis of the results, the sample $LiFePO_4$—S-Micropore displayed similar results, as those found in literature,[46,47] with 0.108% of fading per cycle due to a good physical retention of sulfur polysulfides in the completed microporous structure, but with a relative low initial gravimetric capacity. On the other hand, it is interesting to observe different performance between the samples $LiFePO_4$—S-Corncob and $LiFePO_4$—S-Ketjen although they have the combination of different pore types (micro-meso-macro), but with a different pore size distribution. $LiFePO_4$—S-Corncob shows the highest initial gravimetric capacity, but with high 1.115% of fading per

Table 1. Characterization data of the composite $LiFePO_4$—S samples with different carbon supports. 1.5 M LiTFSI in TMS/TTE was used as electrolyte.

Carbon support	Max. capacity[a] [mAh g^{-1}]	Max. capacity[b] [mAh g^{-1}]	Fading/cycle [%]	CE [%] (50 cycles)	S Charge Plateau [V]	$LiFePO_4$ Charge Plateau [V]
Corncob	698	405	1.115	94.9	2.25	3.49
Micropore	433	217	0.108	97.5	2.26	3.49
Ketjen	634	424	0.264	99.0	2.33	3.56

[a] Considering just the mass of active materials. [b] Considering the total mass of the slurry.

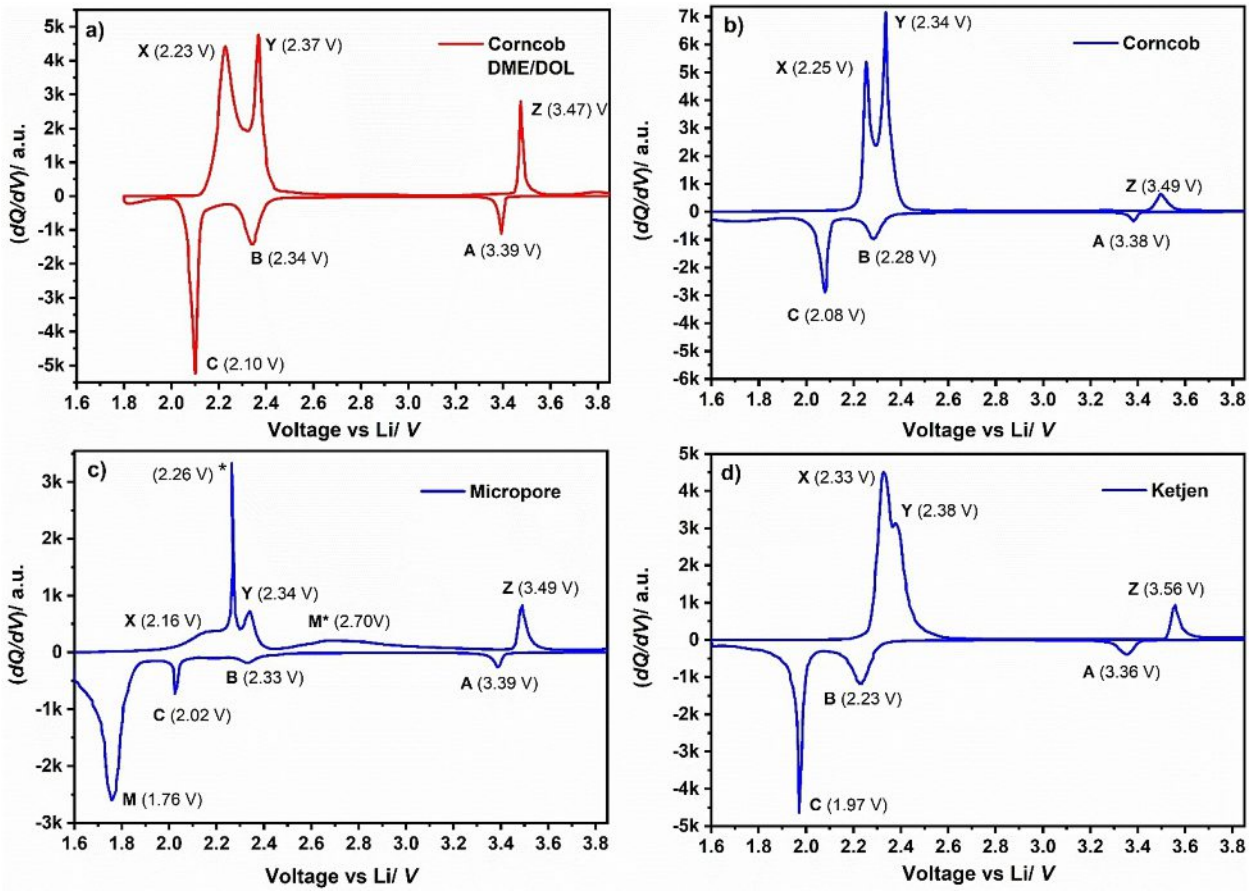

Figure 8. d*Q*/d*V* curves calculated from charge/discharge cycling data of the $LiFePO_4$–S composite cathode with 1.0 M LiTFSI in DME/DOL with a) Corncob carbon and 1.5 M LiTFSI in TMS/TTE with carbons b) Corncob, c) Micropore and d) Ketjen.

cycle, according to table 1. The nature of corncob carbon (sheet-like structure) enhances the wettability in the cathode and reduces delithiation potential of both active materials (2.25 and 3.49 V), as can be noticed in table 1, but this morphology probably is not beneficial for controlling of polysulfides shuttle. Similar behavior has been reported when this carbon derived from biomass was used in Li–S batteries.[48] Despite its beneficial high initial gravimetric capacity and low activation potential, there is a remarkable fading, possibly due to above mentioned natural carbon structure. Homogeneous distribution of micro and mesoporous of commercial Ketjenblack results in a better performance (enough utilization of S and $LiFePO_4$) during the cycling process of the composite even when moderate polarization occurs.

3. Conclusions

The outstanding galvanostatic cycling performance of $LiFePO_4$-sulfur composites in battery half cells with Li as counter electrode revealed that the new cathode concept "two cathodes in one" works appropriately in practical Li-ion batteries. The cell tested with a typical DME/ DOL electrolyte suffers from strong shuttle effect. On the other hand, batteries assembled with the electrolyte with TMS/TTE solvents showed a stable performance of the $LiFePO_4$-sulfur composite. The highest capacity was achieved using Ketjenblack carbon as sulfur support, which confines this material avoiding side reaction products. With this sample, a high capacity retention of about 72%, and 99.1% CE, were achieved after 50 cycles. $LiFePO_4$–S-Micropore cathode, differs from other samples, presenting a combination of two conversion mechanisms that should be further investigated. Electrochemical performance optimization of this new composite cathode could be followed by modulating pore size distribution of the carbon support for sulfur, and by varying the composition of the electrolyte (salt/ solvent), looking for high ionic mobility to the active materials while inhibiting the lithium polysulfide shuttle effect.

Experimental Section

Material fabrication

Different S–C composite materials were used in this work, varying the type of carbon: corncob carbon (Corncob), hierarchical porous Ketjenblack (Ketjen) and a microporous YP carbon (Micropore). Furthermore, $LiFePO_4$ covered with carbon was developed to avoid reaction during operation of the final composite cathode.

Sulfur/Corncob composite

Porous carbon was obtained using corncobs that were carbonized in a tubular furnace with an initial heating rate of 3 °C/min until 600 °C followed by second thermal ramp of 5 °C/min until the final temperature of 1100 °C, that was kept constant for 3 h. Textural (surface area) and electrical (resistivity) properties of resulting carbon were evaluated. The resulting carbon shows low resistivity (4.42 Ω cm), high surface area (1745 $m^2 g^{-1}$) and pore volume of 2.36 $cm^3 g^{-1}$. It showed micro- and mesoporous structure. Sulfur was infiltrated into the carbon matrix (S/C) by melt diffusion method (~56 wt.% in the C/S composite), as reported in literature.[49]

Sulfur/Micropore composite

The carbon material YP-50F, purchased from Kuraray Chemical Co., Ltd has a specific surface area of 1523 $m^2 g^{-1}$ as well as total pore volume of 0.81 $cm^3 g^{-1}$ (microporosity). Sulfur was melt-infiltrated in the carbon matrix (S/C) at 155 °C for 0.5 h under ambient conditions (~50 wt.% in the C/S composite).

Sulfur/Ketjen composite

Ketjenblack EC-600JD, purchased from Akzonobel, is an often-used reference carbon material as well as conductive additive due to its high graphitization degree, with a high conductivity and specific surface area of 1340 $m^2 g^{-1}$ as well as total pore volume of 2.77 $cm^3 g^{-1}$ (micro and mesoporosity). Sulfur was infiltrated in the carbon matrix (S/C) by using melt-infiltration process at 155 °C for 0.5 h under air (~67 wt.% in the C/S composite).

Carbon covered $LiFePO_4$

To avoid reactions between $LiFePO_4$ and sulfur derivatives, $LiFePO_4$ was coated with carbon. This was achieved by hydrothermal carbonization with sucrose, performed at 180 °C in a hydrothermal reactor for 21 h, followed by a thermal treatment at 650 °C under nitrogen atmosphere. Hydrothermal carbon was prepared using acetic acid as reaction medium. Final product $LiFePO_4$–C contains about 50 and 50 wt.%, respectively.

Electrode preparation

The electrodes were prepared by mixing $LiFePO_4$–C, S/C composite, carboxymethyl cellulose (CMC)/styrene-butadiene-rubber (SBR) 1:1 ratio as binder, and multi-walled CNT (Nanocyl 7000) as conductive additive. Water was added to the mixture before stirring, to form a paste, the mixture was milled for 10 min in a vibration mill MM400 from Retsch. The electrode composition of CNT : $LiFePO_4$–S/C : CMC was 15:80:5 ($LiFePO_4$: S/C ratio of 1:1). A layer of the paste was casted onto a carbon-coated aluminum foil sheet of 20 μm (MTI) with a doctor blade (200 μm wet film thickness), then dried at 80 °C for 10 min in a hot air oven and finally dried overnight at room temperature. Circular electrodes with a diameter of 15 mm were punched out. Prior to battery assembly, the cathodes were dried for 2 h at 50 °C in a vacuum oven.

Electrochemical characterization

Coin cells were assembled in an argon filled MBraun glove box with < 0.1 ppm (O_2 and H_2O). Electrochemical characterization was performed in CR2016 coin cells. The half cells were assembled using polyethylene (PE) or polypropylene (PP) separators and a lithium chip (MTI Corp., 16.5 mm diameter and 250 μm thickness) as counter electrode. Experiments were carried out with a moderate electrolyte amount of 7 $\mu L\, mg^{-1}_{comp}$ ether-based 1 M LiTFSI + 0.25 M $LiNO_3$ in DME/DOL (v:v = 1:1) and 1.5 M LiTFSI in TMS/TTE electrolyte. Galvanostatic cycling experiments of all half cells were performed with a BASYTEC CTS test system. The $LiFePO_4$–S cells were operated at a constant rate of C/10 (1 C = 972 $mAh\, g^{-1}_{comp}$) in a voltage range of 1.80–3.85 V (DME/DOL) or 1.60–3.85 V (TMS/TTE). Total gravimetric capacity was calculated considering the average theoretical capacity of both cathode materials. The experimental capacity of $LiFePO_4$, in the composite cathode, was calculated from the beginning of the $LiFePO_4$ plateau of the voltage profile curves. The Coulombic efficiency (CE) was calculated by dividing the discharge (lithiation) capacity by the charge (delithiation) capacity.

Acknowledgements

J.D.G.M. acknowledges the financial support CONACyT through scholarship number 603570, the Project CB-2014-01-243407 and the Energy Storage Network. The support of VIEP-BUAP through the project VIEP2019-100523072 is also acknowledged. The authors also thank Tom Boenke for his support in reviewing this manuscript.

Conflict of Interest

The authors declare no conflict of interest.

Keywords: carbon · composite cathodes · electrochemistry · Li-ion batteries · Li–S batteries

[1] P. G. Bruce, S. A. Freunberger, L. J. Hardwick, J. M. Tarascon, *Nat. Mater.* **2012**, *11*, 19–29.
[2] J. W. Choi, D. Aurbach, *Nat. Rev. Mater.* **2016**, *1*, 16013.
[3] J. D. Garay-Marín, E. Quiroga-González, L. L. Garza-Tovar, *ChemistrySelect* **2020**, *5*, 6172–6177.
[4] J. B. Goodenough, Y. Kim, *Chem. Mater.* **2009**, *22*, 587–603.
[5] J. Wu, W. Cai, G. Shang, *Nanoscale Res. Lett.* **2016**, *11*, 223.
[6] S. Franger, C. Bourbon, F. Le Cras, *J. Electrochem. Soc.* **2004**, *151*, A1024–A1027.
[7] H. Ni, J. Liu, L.-Z. Fan, *Nanoscale* **2013**, *5*, 2164–2168.
[8] S. B. Lee, S. H. Cho, V. Aravindan, H. S. Kim, Y. S. Lee, *Bull. Korean Chem. Soc.* **2009**, *30*, 2223–2226.
[9] J. Yan, X. Liu, B. Li, *Adv. Sci.* **2016**, *3*, 160010.
[10] S. Chen, Y. Gao, Z. Yu, M. L. Gordin, J. Song, D. Wang, *Nano Energy* **2017**, *31*, 418–423.
[11] W. Ren, W. Ma, S. Zhang, B. Tang, *Energy Storage Mater.* **2019**, *23*, 707–732.
[12] C. S. Kim, A. Guerfi, P. Hovington, J. Trottier, C. Gagnon, F. Barray, A. Vijh, M. Armand, K. Zaghib, *Electrochem. Commun.* **2013**, *32*, 35–38.
[13] A. Berger, A. T. S. Freiberg, A. Siebel, R. Thomas, M. U. M. Patel, M. Tromp, H. A. Gasteiger, Y. Gorlin, *J. Electrochem. Soc.* **2018**,165, A1288–A1296.
[14] W. Li, G. Zheng, Y. Yang, Z. W. Seh, N. Liu, Y. Cui, *Proc. Mont. Acad. Sci.* **2013**, *110*, 7148–7153.
[15] S. Risse, N. A. Cañas, N. Wagner, E. Härk, M. Ballauff, K. A. Friedrich, *J. Power Sources* **2016**, *323*, 107–114.
[16] J. Scheers, S. Fantini, P. Johanss, *J. Power Sources* **2014**, *255*, 204–218.
[17] K. Okada, I. Kimura K Machida, *RSC Adv.* **2018**, *8*, 5848.
[18] J. Ming, M. Li, P. Kumar, A.-Y. Lu, W. Wahyudi, L.-J. Li, *ACS Energy Lett.* **2016**, *1*, 529–534.

[19] W. Bo, J. Fan, X. Ying, L. Hao, W. Fei, R. Tingting, W. Dianlong, Z. Yu, D. Shixue, *Energy Storage Mater.* **2020**, *26*, 433–442.
[20] Y. Ye, W. Bo, S. Rensheng, W. Fei, L. Hao, G. Tiantian, W. Dianlong, *New J. Chem.* **2018**, *42*, 6626–6630.
[21] D. Aurbach, E. Zinigrad, H. Teller, Y. Cohen, G. Salitra, H. Yamin, P. Dan, E. Elster, *J. Electrochem. Soc.* **2002**, *149*, A1267.
[22] E. Zinigrad, E. Levi, H. Teller, G. Salitra, D. Aurbach, P. Dan, *J. Electrochem. Soc.* **2004**, *151*, A111.
[23] A. Rosenman, E. Markevich, G. Salitra, D. Aurbach, A. Garsuch, F. Francois Chesneau, *Adv. Energy Mater.* **2015**, *5*, 1500212.
[24] S. S. Zhang, *Electrochim. Acta* **2012**, *70*, 344–348.
[25] Y. Matsumae, K. Obata, A. Ando, M. Yanagi, Y. Kamei, K. Ueno, K. Dokko, M. Watanabe, *Electrochemistry* **2019**, *87*, 254–259.
[26] C. Weller, S. Thieme, P. Härtel, H. Althues, S. Kaskel, *J. Electrochem. Soc.* **2017**, *164*, A3766–A3771.
[27] M. Piwko, S. Thieme, C. Weller, H. Althues, S. Kaskel, *J. Power Sources* **2017**, *362*, 349–357.
[28] H. Pan, J. Chen, R. Cao, V. Murugesan, N. N. Rajput, K. Sung Han, et al., *Nat. Energy* **2017**, *2*, 813–820.
[29] J. Schuster, G. He, B. Mandlmeier, T. Yim, K. Tae Lee, T. Bein, L. F. Nazar, *Angew. Chem. Int. Ed.* **2012**, *51*, 3591–3595; *Angew. Chem.* **2012**, *124*, 3651–3655.
[30] C. Zhang, H. B. Wu, C. Yuan, Z. Guo, X. W. Lou, *Angew. Chem. Int. Ed.* **2012**, *51*, 9592–9595.
[31] Y. Cao, X. Li, I. A. Aksay, J. Lemmon, Z. Nie, Z. Yang, J. Liu, *Phys. Chem. Chem. Phys.* **2011**, *13*, 7660–7665.
[32] G. Zhou, S. Pei, L. Li, D. W. Wang, S. Wang, K. Huang, L. C. Yin, F. Li, H. M. Cheng, *Adv. Mater.* **2014**, *26*, 625–631.
[33] G. Zheng, Y. Yang, J. J. Cha, S. S. Hong, Y. Cui, *Nano Lett.* **2011**, *11*, 4462–4467.
[34] G. Zheng Q Zhang, J. J. Cha, Y. Yang, W. Li, Z. She, Y. Cui, *Nano Lett.* **2013**, *13*, 1265–1270.
[35] Z. W. Seh, W. Li, J. J. Cha, G. Zheng, Y. Yang, M. T. McDowell, P.-C. Hsu, Y. Cui, *Nat. Commun.* **2013**, *4*, 1331.
[36] Q. Pang, D. Kundu, M. Cuisinier, L. F. Nazar, *Nat. Commun.* **2014**, *5*, 4759.
[37] C. Kensy, P. Härtel, J. Maschita, S. Dörfler B Schumm, T. Abendroth, H. Althues, B. V. Lotsch, S. Kaskel, *Carbon* **2020**, *161*, 190–197.
[38] R. Fang, S. Zhao, Z. Sun, D. W. Wang, H. M. Cheng, F. Li, *Adv. Mater.* **2017**, *29*, 1606823.
[39] Y. Wu, T. Momma, S. Ahn, T. Yokoshima, H. Nara, T. Osaka, *J. Power Sources* **2017**, *366*, 65–71.
[40] X. B. Cheng, J. Q. Huang, H. J. Peng, J. Q. Ni, X. Y. Liu, Q. Zhang, F. Wei, *J. Power Sources* **2014**, *253*, 263–268.
[41] S. S. Zhang, *J. Power Sources* **2013**, *231*, 153–162.
[42] Y. Diau, K. Xie, S. Xiong, X. Hong, *J. Power Sources* **2013**, *235*, 181–186.
[43] L. Jannelli, A. Inglese, A. Sacco, P. Ciani, *Z. Naturforsch.* **1975**, *30* a, 87–91.
[44] Q. Zou, Y. C. Lu, *J. Phys. Chem. Lett.* **2016**, *7*, 1518–1525.
[45] E. Markevich, G. Salitra, Y. Talyosef, F. Chesneau, D. Aurbach, *Journal of The J. Electrochem. Soc.* **2017**, *164*, A6244–A6253.
[46] S. Xin, L. Gu, N. H. Zhao, Y. X. Yin, L. J. Zhou, Y. G. Guo, L. J. Wan, *J. Am. Chem. Soc.* **2012**, *134*, 18510–18513.
[47] R. Elazari, G. Salitra, A. Garsuch, A. Panchenko, D. Aurbach, *Adv. Mater.* **2011**, *23*, 5641.
[48] J. Guo, J. Zhang, F. Jiang, S. Zhao, Q. Su, G. Du, *Electrochim. Acta* **2015**, *176*, 853–860.
[49] X. Ji, K. T. Lee, L. F. Nazar, *Nat. Mater.* **2009**, *8*, 500–506.

Manuscript received: October 9, 2020
Revised manuscript received: November 2, 2020
Accepted manuscript online: November 4, 2020
Version of record online: November 18, 2020